arXiv:1403.0161v1 [astro-ph.HE] 2 Mar 2014

Milagro Observations of Potential TeV Emitters

A. A. Abdo[a,p], A. U. Abeysekara[a], B. T. Allen[b,q], T. Aune[c,r], A. S. Barber[a,s], D. Berley[d], J. Braun[d], C. Chen[b], G. E. Christopher[e], T. DeYoung[f], B. L. Dingus[g], R. W. Ellsworth[h], M. M. Gonzalez[i], J. A. Goodman[d], E. Hays[j], C. M. Hoffman[g], P. H. Hüntemeyer[k], A. Imran[g], B. E. Kolterman[e], J. T. Linnemann[a], J. E. McEnery[j], T. Morgan[l], A. I. Mincer[e], P. Nemethy[e], J. Pretz[g], J. M. Ryan[l], P. M. Saz Parkinson[c,o], M. Schneider[m], A. Shoup[n], G. Sinnis[g], A. J. Smith[d], V. Vasileiou[d,u], G. P. Walker[g,t], D. A. Williams[c], G. B. Yodh[b]

[a] *Department of Physics and Astronomy, Michigan State University, BioMedical Physical Sciences Building, East Lansing, MI 48824*
[b] *Department of Physics and Astronomy, University of California, Irvine, CA 92697*
[c] *Santa Cruz Institute for Particle Physics, University of California, 1156 High Street, Santa Cruz, CA 95064*
[d] *Department of Physics, University of Maryland, College Park, MD 20742*
[e] *Department of Physics, New York University, 4 Washington Place, New York, NY 10003*
[f] *Department of Physics, Pennsylvania State University, University Park, PA 16802*
[g] *Group P-23, Los Alamos National Laboratory, P.O. Box 1663, Los Alamos, NM 87545*
[h] *Department of Physics and Astronomy, George Mason University, 4400 University Drive, Fairfax, VA 22030*
[i] *Instituto de Astronomía, Universidad Nacional Autónoma de México,D.F., México, 04510*
[j] *NASA Goddard Space Flight Center, Greenbelt, MD 20771*
[k] *Department of Physics, Michigan Technological University, Houghton, MI 49931, USA*
[l] *Department of Physics, University of New Hampshire, Morse Hall, Durham, NH 03824*
[m] *University of California Santa Cruz, Natural Science 2, 1156 High Street, Santa Cruz, CA 95064, USA*
[n] *Ohio State University, Lima, OH 45804*
[o] *Department of Physics, The University of Hong Kong, Pokfulam Road, Hong Kong, China*
[p] *Current address: Operational Evaluation Division, Institute for Defense Analyses, 4850 Mark Center Drive, Alexandria, VA 22311-1882*
[q] *Current address: Harvard-Smithsonian Center for Astrophysics, Cambridge, MA 02138*
[r] *Current address: Department of Physics and Astronomy, University of California, Los Angeles, CA 90095*
[s] *Current address: Department of Physics, University of Utah, Salt Lake City, UT 84112*
[t] *Current address: National Security Technologies, Las Vegas, NV 89102*
[u] *Current address: Laboratoire Univers et Particules de Montpellier, Université Montpellier 2, CNRS/IN2P3, CC 72, Place Eugène Bataillon, F-34095 Montpellier Cedex 5, France*

Abstract

This paper reports the results from three targeted searches of Milagro TeV sky maps: two extragalactic point source lists and one pulsar source list. The first extragalactic candidate list consists of 709 candidates selected from the *Fermi-LAT* 2FGL catalog. The second extragalactic candidate list contains 31 candidates selected from the TeVCat source catalog that have been detected by imaging atmospheric Cherenkov telescopes (IACTs). In both extragalactic candidate lists Mkn 421 was the only source detected by Milagro. This paper presents the Milagro TeV flux for Mkn 421 and flux limits for the brighter *Fermi-LAT* extragalactic sources and for all TeVCat candidates. The pulsar list extends a previously published Milagro targeted search for Galactic sources. With the 32 new gamma-ray pulsars identified in 2FGL, the number of pulsars that are studied by both *Fermi-LAT* and Milagro is increased to 52. In this sample, we find that the probability of Milagro detecting a TeV emission coincident with a pulsar increases with the GeV flux observed by the *Fermi-LAT* in the energy range from 0.1 GeV to 100 GeV.

Keywords: astroparticle physics, pulsars, galaxies, active galactic nuclei, gamma-rays

*Corresponding author: udaraabeysekara@yahoo.com

1. Introduction

The Milagro gamma-ray observatory was a water Cherenkov detector located near Los Alamos, New Mexico, USA at latitude 35.9° north, longitude 106.7° west and altitude 2630 m [4]. Milagro recorded data from 2001-2008 and was sensitive to extensive air showers initiated by gamma-rays with energies from a few hundred GeV to ∼100 TeV. Unlike atmospheric Cherenkov telescopes, Milagro had a wide field of view and it was able to monitor the sky with a high duty cycle($> 90\%$).

The Milagro collaboration has performed blind source searches and found a number of TeV sources ([13] and [1] We refer to this as Milagro Galactic Plane Surveys). Blind searches for excess events over the full sky have a high probability of picking up random fluctuations. Therefore, after trials correction, a full sky blind search is less sensitive than searches using a smaller predefined list of candidates. The *Fermi Large Area Telescope (Fermi-LAT)* collaboration published such a list known as the Bright Source List or 0FGL list [2]. In a previous publication, Milagro reported a search using 0FGL sources identified as Galactic sources [3], which we will refer to as the Milagro 0FGL paper.

We report here two Milagro targeted searches for extragalactic sources. The first extragalactic candidate list is compiled from the extragalactic sources in the 2FGL catalog[23]. The analysis presented in this paper looks for the TeV counterparts of these sources. The second extragalactic candidate list is made from the TeVCat catalog [25] of extragalactic sources. While TeVCat detections may include transient states of variable extragalactic sources, this search looks for long-term time averages by integrating over the full Milagro data set. However, it is not appropriate to use the second extragalactic candidate list to perform a population study as it has candidates detected from several instruments with different sensitivities.

Our previous Milagro 0FGL publication found that the *Fermi-LAT* bright sources that were measured at or above 3 standard deviations in significance (3σ) by Milagro were dominated by pulsars and/or their associated pulsar wind nebulae (PWN). Therefore, in this paper we extend the previous Galactic search by making a candidate list from the pulsars in the 2FGL source list, and search for TeV emission from the sky locations of gamma-ray pulsars detected by the *Fermi-LAT*. The angular resolution of Milagro ($0.35° < \delta\theta < 1.2°$) is not sufficient to distinguish the PWN from the pulsar.

2. Methodology

2.1. Construction Of Candidate Lists

The first candidate list, which will be referred to as the 2FGL Extragalactic List, is derived from the 2FGL catalog by looking for sources off the Galactic plane ($|b| > 10°$) that have no association with pulsars. There are 709 *Fermi-LAT* sources within Milagro's sky coverage ($-7°$ <DEC< $80°$), of which 72% are associated with blazars. Among these blazars 4 are firmly identified as BL Lac[1] blazars and 12 are firmly identified as FSRQ[2] type of blazars.

The second extragalactic candidate list, which we will call the TeVCat Extragalactic List, is taken from TeVCat, an online gamma-ray source catalog (http://tevcat.uchicago.edu). As of February 8th, 2012 it contained 135 sources, of which 31 were located off the Galactic plane and within Milagro's sky coverage. These 31 sources were all detected with Cherenkov telescopes and 23 are identified as BL Lac objects.

There are 52 sources in the 2FGL catalog associated with pulsars which are in the Milagro's sky coverage. Twenty of these pulsars were already considered as candidates in the Milagro 0FGL publication. So the third candidate list, which will be called the Pulsar List, consists of only the 32 new pulsars. Of these, 17 were identified as pulsars by pulsations seen in *Fermi-LAT* data and the remaining 15 sources were labeled as pulsars in 2FGL because of their spatial association with known pulsars.

[1] BL Lac is a type of active galaxy of known to be strongly γ-ray emitting objects [15].
[2] Flat Spectrum Radio Quasar

2.2. Spectral Optimizations

In order to optimize the sensitivity to photon sources, Milagro sky maps are constructed by plotting the location for each event with a weight based on the relative probability of it being due to a primary photon or hadron [4]. The weight calculation depends on the assumed photon spectrum and can be suboptimal (but not incorrect) if the weight optimization hypothesis is considerably different from the actual source spectrum. The weights are therefore optimized separately for two hypotheses.

For the extragalactic candidate lists, a power law with spectral index α= -2.0 with a 5 TeV exponential cut-off ($E^{-2.0}e^{-\frac{E}{5\mathrm{TeV}}}$) was assumed. This choice reflects the fact that when TeV gamma-rays travel cosmological distances they are attenuated due to interactions with photons from the extragalactic background light [16] with the result that the energy spectrum of extragalactic sources cut off at high energies. This spectral assumption is also similar to the power law spectral index and the cut-off energy measured for Mkn 421 and Mkn 501 by [20]. However, the choice of 5 TeV cut off might reduce the sensitivity of Milagro to the AGNs with lower cut off energies. For the Pulsar List, a power law with spectral index $\alpha = -2.6$ with no TeV cut-off is used, as was done for the previous Milagro 0FGL and Galactic Plane Survey papers.

2.3. Source Detection Technique

The expected significance at a sky location with no true emission is a Gaussian random variable with mean 0 and unit standard deviation [13]. A common treatment of N candidate searches is to use a trials correction technique. Here one choose a significance threshold, calculate the tail probability (p-value) λ, and adjusts the p-value threshold to $\frac{\lambda}{N}$. The purpose of the trials correction is to maintain, at the value λ, the probability of a background fluctuation producing one or more false discoveries among the N searches.

The False Discovery Rate (FDR) technique discussed in [22] offers some advantages over the trials correction technique. Instead of controlling the expected probability of having even one false detection, FDR controls the *expected fraction* of false discoveries among a set of detections; that is, it controls the contamination fraction of the *lists* of associations, rather than the probability of a random individual association being accepted[3]. The key input parameter is again a probability λ, but now λ represents the expected fractional contamination of any announced set of detections. Based on this input parameter, the method dynamically adjusts the detection threshold but in a way that depends on the properties of the entire list of search significances (converted into p-values). This dynamic adjustment is sensitive to whether the distribution of p-values is flat (as would be expected if there were no detectable sources) or skewed to small p-values (i.e. large significances). This adjustment lowers the significance threshold for detection if a list is a "target-rich environment" in such a way that the expected fraction of false discoveries among the announced detections remains at the fraction λ. In particular, the most significant candidate is required to have a p-value of λ/N just as in the trials-correction method, but the n-th most significant candidate need only have a p-value less than $\lambda \times n/N$. As a result, this technique has a higher efficiency for finding real detections, while producing the same results as a trials-correction method in target-poor environments where the only decision is whether to report zero or one detections. The method adjusts for both the length of the search list and the distribution of the significances found within the search lists. However, we note that as a result, a given candidate location might pass the FDR criteria on one search list, but fail in another. We also emphasize that λ controls the *expected* contamination, *i.e.* averaged over potential lists of associations, not the contamination fraction on a specific list[4]. The reader is referred to [22] for further details of the method[5]. In the [3] paper for the Galactic-oriented search with N = 35, a criterion of 3σ was used but it was also found that an FDR criterion of $\lambda = 0.01$ produced the same list of associations. Specifying λ rather than a σ threshold also allows using a single criterion for treating each of the search lists. The analyses presented in

[3]The required calculations are quite simple and can be implemented in a spreadsheet after the significances of the searches on a list are calculated.

[4]For example, in an environment with no real sources, one expects to report an empty list $(1 - \lambda) \times 100\%$ of the time, and about $\lambda \times 100\%$ of the time one would report a list having at least a single (false) candidate

[5]We assume that the search points are uncorrelated, as the angular separations between target locations are normally much more widely seperated than the Milagro point spread function.

this paper uses $\lambda = 0.01$ for defining a TeV association for all our search lists, but significance thresholds are also tabulated in Table 4 for $\lambda = 0.1, 0.05$, and 0.001 so that readers can choose the potential contamination level of candidate lists. Specific candidates passing looser cuts are also denoted as footnotes to the search list tables.

2.4. Stacking Methodology

The FDR technique can be used to search for individual candidates with a TeV association. A stacking analysis can be used to search for evidence of collective TeV emission among the undetected candidates by studying their mean flux. This paper uses the stacking methodology of Section 3 in [21]. The significance of the stacked flux is given by Equation 1 below.

$$\text{Significance} = \frac{\langle \text{I} \rangle}{\sqrt{\vee(\langle \text{I} \rangle)}}, \tag{1}$$

where $\langle I \rangle$ is the weighted average flux as defined in Equation 2 below and $\vee\langle I \rangle$ is its variance, defined in Equation 3.

$$\langle I \rangle = \frac{\sum \frac{I_i}{\sigma_i^2}}{\sum \frac{1}{\sigma_i^2}} \tag{2}$$

$$\vee \langle I \rangle = \frac{\sum \frac{1}{\sigma_i^2}}{\sum \left(\frac{1}{\sigma_i^2}\right)^2} \tag{3}$$

Here I_i is the flux of each candidate and σ_i is the standard deviation of flux of each candidate.

2.5. Flux Calculation

The flux calculation involves a convolution of the Milagro effective area as a function of energy using an assumed energy spectrum, so the flux has some dependence on the assumed energy spectrum. This dependence is greatly reduced when the flux is calculated at the median energy of the detected gamma-ray events at the declination of a source [3]. Therefore, we report the flux at approximately the median energy. Using a similar argument to that in the Milagro 0FGL paper, the flux is derived at 35 TeV for the Pulsar List. For the extragalactic spectral assumption the median energy varies between 6 and 11 TeV, and we choose 7 TeV to report the flux for extragalactic source candidates.

In this paper, we report the flux for the candidates with TeV associations that are identified by the FDR procedure. For the remaining candidates we report flux upper limit. In all cases, the flux and significance calculations are performed assuming that the target is a point-like source. The fluxes are calculated from the excess number of photons above background integrating over a Gaussian point spread function[6] for a point source at the sky position given by the catalog used to compile the list. This approach is similar to that described in the Milagro Galactic Plane Survey papers. The upper limits on the flux are determined using the method described in [19] and are based on an upper limit on the number of excess photons with a 95% confidence limit. The flux upper limit corresponding to a zero excess is called the expected flux limit. The declination dependence of the expected flux limits shown in Figures 1 and 2 are based on Milagro maps made with the spectral optimizations $dN/dE \propto E^{-2.6}$ and $dN/dE \propto E^{-2.0} e^{-\frac{E}{5TeV}}$, respectively. The searches presented in this paper did not examine the whole sky. Another publication is in progress to produce all-sky flux limits from Milagro.

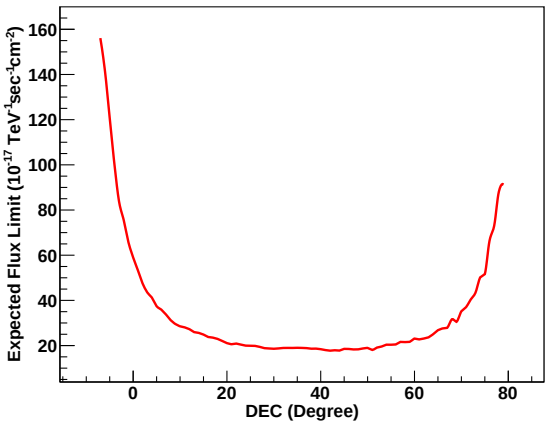

Figure 1: The expected 95% confidence level flux upper limit for Galactic sources corresponding to zero excess derived at 35 TeV for each declination band of the Milagro sky maps made with spectral assumption $dN/dE \propto E^{-2.6}$.

3. Results

In the 2FGL Extragalactic List only 2FGL J1104.4+3812 (also known as Mkn 421) is classified as a source by the FDR procedure with our standard $\lambda = 0.01$ cut. Figure 3 shows the region in the Milagro sky map around Mkn 421. From the 2FGL Extragalactic candidate list the fluxes or the 95% confidence level flux upper limits for the brightest 20% of the 2FGL candidates in the 3 GeV to 10 GeV energy band is given in Table 1. From the TeVCat Extragalactic List only Mkn 421 is classified as a source by the FDR procedure with our standard $\lambda = 0.01$. The results with our standard FDR cut of $\lambda = 0.01$ are summarized in Table 2.

Results from the source search in the Pulsar List are summarized in Table 3. In this list, the FDR procedure with $\lambda = 0.01$ classified 3 GeV pulsars (2FGL J2238.4+5902, 2FGL J2030.0+3640 and 2FGL J1928.8+1740c) as having coincident TeV emission. Figure 4 shows the regions of the Milagro sky maps around those candidates. The brighter area near 2FGL J2238.4+5902 (Figure 4(a)) corresponds to 0FGL J2229.0+6114, and it is also associated with the bright TeV source MGRO J2228+61 [18]. The Milagro flux at the location of 0FGL J2229.0+6114 was published in the Milagro 0FGL paper. Similarly 2FGL J2030.0+3640 (Figure 4(b)) is located near a brighter area which belongs to 0FGL J2020.8+3649. The Milagro flux at this 0FGL source location was also published in the Milagro 0FGL paper. Follow-up observations by TeV instruments with better angular resolution could clarify the TeV emission structure in both of these regions; some initial studies of this region have been already done [[5], [14]]. 2FGL J2030.0+3640 also has a spatial association with the Milagro candidate named as C3 in [1]. Milagro candidate C3 is measured at RA = 307.75^0 and DEC = 36.52^0 with extent diameter of 2.8^0 [1].

To assess how likely it would be to observe TeV emission coincident with 2FGL sources associated with pulsars if they arose from statistical fluctuations in the Milagro data, we calculate the probability that a set of 32 random points in the Milagro Galactic plane ($|l| < 10^0$) would have 3 or more FDR associations. For a simulated background-only sky (consisting of a standard normal significance distribution) the probability of finding 3 or more associations is 1×10^{-6}. Thus finding 3 associations would be a 4.3 σ fluctuation for random points on a background-only sky. As expected, the $\lambda = 0.01$ FDR cut yields no associations 99% of the time with random locations on a random sky (with no real sources). However, the probability of finding 3 or more associations from random lists of 32 locations within the actual Milagro Galactic plane $|l| < 10^0$ (which contains TeV sources) is 0.01. This is much higher than for a background-only sky, so

[6]The width of the Gaussian point spread function is a function of the estimated energy of each event and varies between 0.3° and 0.7°.

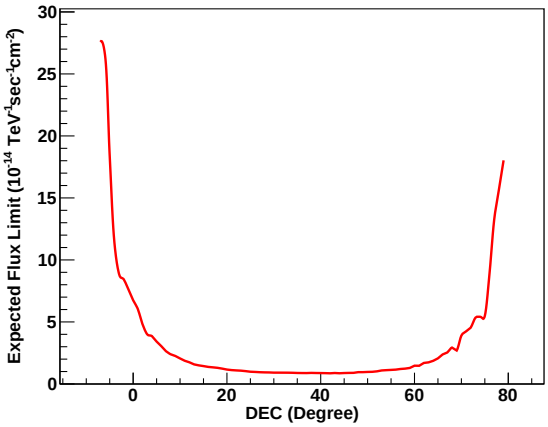

Figure 2: The expected 95% confidence level upper limit on the flux for extragalactic sources corresponding to zero excess derived at 7 TeV for each declination band of the Milagro sky maps made with spectral assumption $dN/dE \propto E^{-2.0}e^{-\frac{E}{5TeV}}$.

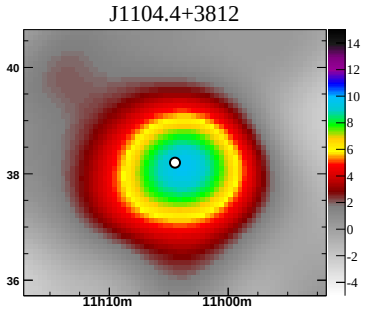

Figure 3: This map shows the $5^\circ \times 5^\circ$ (25 minutes $\times$ 5°) region around Mkn 421. The LAT source position is marked by a white dot. This map is made with the spectral optimization $dN/dE \propto E^{-2.0}e^{-\frac{E}{5TeV}}$ and the data have been smoothed using a Gaussian function. The color of a bin shows the statistical significance (in standard deviations) of that bin. The horizontal axis is right ascension in hours and the vertical axis is declination in degrees.

that reporting 3 associations in the Milagro Galactic plane data would be a 2.3 σ fluctuation if we were starting from a randomly located candidate list (rather than seeking associations with the 2FGL pulsar list).

By varying λ the reader can construct alternative target lists with different contamination fractions, to assess how clearly candidates have passed a given association criterion. Table 4 summarizes the FDR significance thresholds for each of the lists we have searched using $\lambda = 0.1, 0.05, 0.01$ and 0.001. The table also gives the significance thresholds which would have resulted from the trials correction technique. The comparison between the FDR and the trials corrections thresholds allows assessment of how much the FDR procedure has lowered the significance threshold in response to evidence of associations.

So far our results have focused on individual candidates with a TeV association. We also searched for evidence of collective TeV emission on the candidates that fail the $\lambda = 0.01$ FDR cut by using the stacking method described in section 2.4 . We stacked 2FGL Extragalactic candidates in two different ways: first all FDR False 2FGL Extragalactic sources and then the FDR False sources among the brightest 20% in the *Fermi-LAT* energy band 3-10 GeV. These two lists had 0.7σ and 0.6σ significance collectively. Stacking of TeV Cat candidates other than Mkn 421 has only a slightly more positive upward fluctuation of 0.9σ . The rejected pulsar candidates have a -0.5σ fluctuation from the background. None of these stacking results

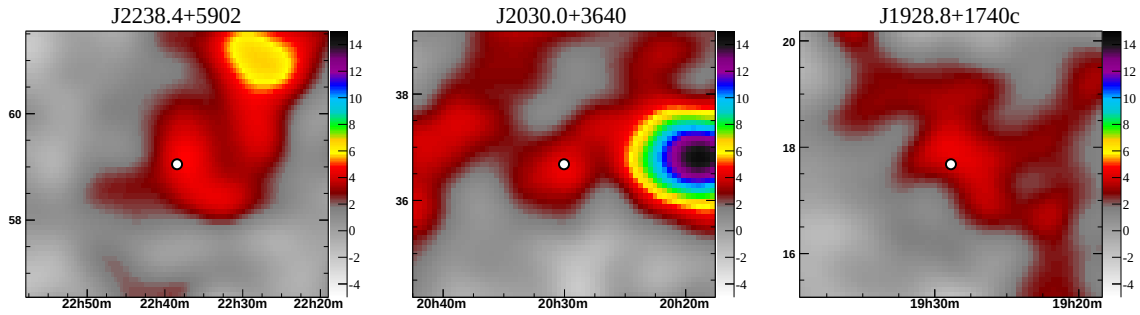

(a) (b) (c)

Figure 4: These maps show the $5^\circ \times 5^\circ$ (25 minutes $\times$ 5°) region around 2FGL J2238.4+5902, 2FGL J2030.0+3640 and 2FGL J1928.8+1740c. The LAT source positions are marked by white dots. These maps are made with the spectral optimization $dN/dE \propto E^{-2.6}$ and the data have been smoothed using a Gaussian function. The color of a bin shows the statistical significance (in standard deviations) of that bin. The horizontal axis is right ascension in hours and the vertical axis is declination in degrees.

indicate significant collective gamma-ray emission from the rejected candidates.

4. Discussion

Mkn 421 is the only source that is classified as a TeV source in both extragalactic lists. Milagro also observed a signal excess at the sky locations of Mkn 501, TXS 1720+102 and 1ES 0502+675 . Their significances are 2.93, 2.84 and 2.53 respectively, which is insufficient to pass our standard FDR cut of $\lambda = 0.01$. Among these three candidates Mkn 501 and 1ES 0502+675 have been already reported as TeV sources in TevCat. However TXS 1720+102 has not yet been identified as a source with TeV emission. This is a radio quasar type blazar identified at a redshift of 0.732 [10]. The lowest FDR cut that TXS 1720+102 passes is $\lambda = 0.32$. With this loose FDR cut, three candidates become TeV associations: Mkn 421, Mkn 501 and TXS 1720+102. However, the expected contamination of the resulting candidates list is 32% so it is likely that TXS 1720+102 is a background fluctuation. While it is hard to advocate a dedicated IACT observation of TXS 1720+102, better observations will be performed by the High Altitude Water Cherenkov (HAWC) survey instrument [6], which is already started to operate at a sensitivity better than Milagro.

In this paper we presented the TeV flux/flux limit measurements at 32 sky locations of 2FGL sources marked as pulsars. At the time we wrote this paper, none of these 2FGL pulsars were reported as detections in the TeVCat or in the H.E.S.S. source catalog. However, TeV flux upper limits of some these sources have been measured by IACTs. For an example, the flux upper limit of PSR J1928+1746 was measured by the VERITAS observatory [7], which is associated with the 2FGL J1928.8+1740c. VERITAS observed a $+1.2\sigma$ significance at this pulsar position and 99% confidence flux upper limit of 2.6×10^{-13} cm^{-2}s^{-1} above 1 TeV was measured assuming a power-law spectrum with power law index -2.5. Contrasted with this measurement, Milagro measured a $46.41 \pm 11.5 \times 10^{-17}$ photons TeV^{-1}s^{-1}cm^{-2} of flux at 35 TeV from this pulsar position, assuming a power-law spectrum with power law index -2.6. The Milagro flux measurement is order of magnitude larger than the VERITAS upper limit. This difference may be caused by the wider point spread function of Milagro compared with that of VERITAS ($\sim 0.11^\circ$[7]). Therefore, the Milagro flux may include some additional diffuse emission or emission from unresolved point sources that is not contained within the VERITAS point spread function. We also compared our flux/flux limit measurements with the H.E.S.S. Galactic Plane Survey [17], and found that our measurements are consistent with the H.E.S.S. measurements.

The Milagro 0FGL paper reported the Milagro flux/flux limit at the locations of 16 bright *Fermi-LAT* sources from the 0FGL catalog that were associated with pulsars. Among these 16 pulsars, 9 passed the

standard FDR cut of $\lambda = 0.01$. 0FGL J2055.5+2540, 0FGL J2214.8+3002 and 0FGL J2302.9+443 were categorized as sources with unknown source type and 0FGL J1954.4+2838 was identified as a source with a spatial association with a known supernova remnant. In the 2FGL catalog these four sources have been identified as pulsars and only 0FGL J1954.4+2838 passed our standard FDR cut. Therefore all together 52 pulsars detected by *Fermi-LAT* have been observed by Milagro and 13 pulsars were identified with TeV associations. We use this sample to study the correlation between GeV and TeV flux.

Figure 5 shows the TeV flux measured by Milagro vs the GeV flux measured by *Fermi-LAT* for these 52 pulsars. Data points marked with red triangles are Milagro upper limits measured at the sky locations of the candidates that failed the $\lambda = 0.01$ FDR cut. Blue data points represents the Milagro flux at the sky locations of the candidates that passed the $\lambda = 0.01$ FDR cut. The Milagro flux/flux limits used in this plot were derived assuming the targets are point sources. However, some of these objects are extended sources, for which the point source flux would underestimate the total flux. Geminga is a specific example, as seen in the Milagro 0FGL paper. In Figure 5 Geminga is circled in red.

We can also study how the fraction of pulsars with a TeV counterpart changes as a function of the GeV flux. We define F_T as the fraction of pulsars that passed our standard FDR cut in a given bin of GeV flux.

$$F_T = \frac{\text{Number of FDR true candidates in a given flux bin}}{\text{Total number of candidates in a given flux bin}} \tag{4}$$

As shown in Figure 6 F_T clearly increases with the *Fermi-LAT* flux. Both the F_T plot and the flux correlation plot strongly prefer a dependence on the GeV flux. Therefore we have evidence that pulsars brighter in the GeV energy range are more likely to have a detectable TeV counterpart than pulsars fainter in the GeV energy range. Further analysis of the GeV-TeV correlation is in progress and will be published in a follow-up paper.

5. Conclusions

We present a targeted search for extragalactic sources in the Milagro data using a list of bright 2FGL extragalactic sources and TeV sources from the TeVCat catalog as targets. Using the FDR procedure with $\lambda = 0.01$, we find that Mkn 421 is the only extragalactic TeV source detected by Milagro. There is no evidence of collective TeV emission seen from the remaining extragalactic candidates.

The analysis performed in the Milagro 0FGL paper has been extended by searching for TeV emission at the locations of 32 additional *Fermi-LAT* detected pulsars. TeV emission has been found associated with three of them: 2FGL J2238.4+5902, 2FGL J2030.0+3640 and 2FGL J1928.8+1740c. The first two of these are near bright VHE sources previously reported as being associated with energetic pulsars in the 0FGL catalog. They might benefit from a higher spatial resolution TeV follow-up to study the emission structure from the two nearby source regions. The pulsar candidates that failed the $\lambda = 0.01$ FDR cuts were studied in a stacking analysis but did not show any collective TeV emission. Finally, we presented evidence that pulsars brighter in the GeV energy range are more likely to have a detectable TeV counterpart.

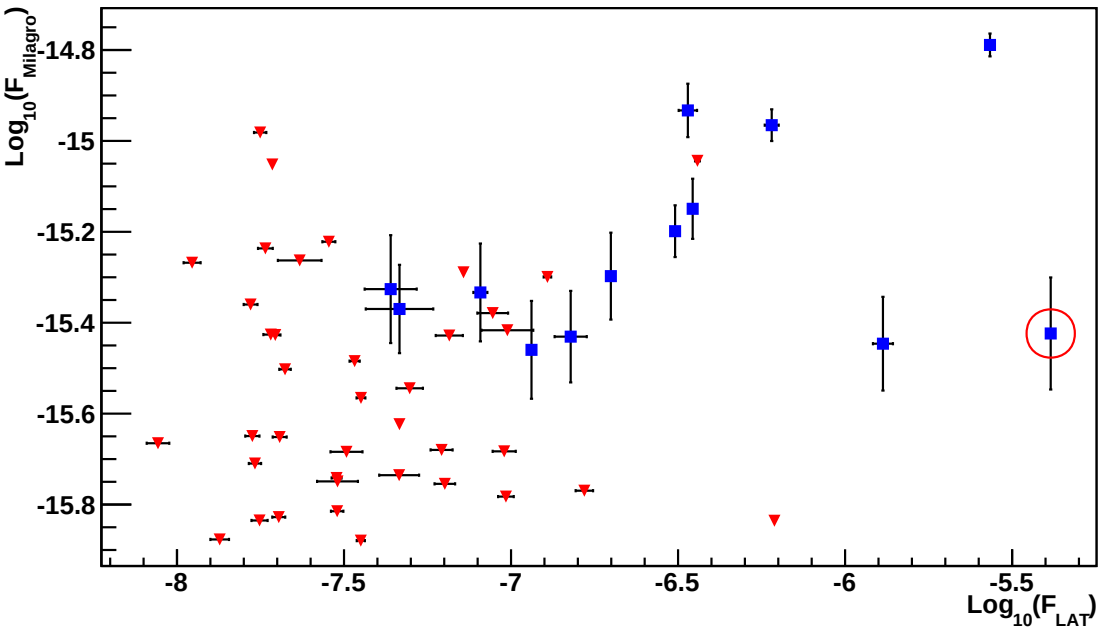

Figure 5: The horizontal axis is the *Fermi-LAT* flux (photons $s^{-1}cm^{-2}$), integrated over the energy range from 100 MeV to 100 GeV. The vertical axis is the Milagro flux derived at 35 TeV (photons $TeV^{-1}s^{-1}cm^{-2}$), assuming all targets are point sources. Red data points are Milagro upper limits of candidates that failed the $\lambda = 0.01$ FDR cut. Blue data points are the Milagro flux derived for the candidates that passed the $\lambda = 0.01$ FDR cut. The Milagro flux/flux limits used in this plot were derived assuming the targets are point sources. However, some of these objects are extended sources, for which the point source flux would underestimate the total flux. Geminga is a specific example and it is circled in red.

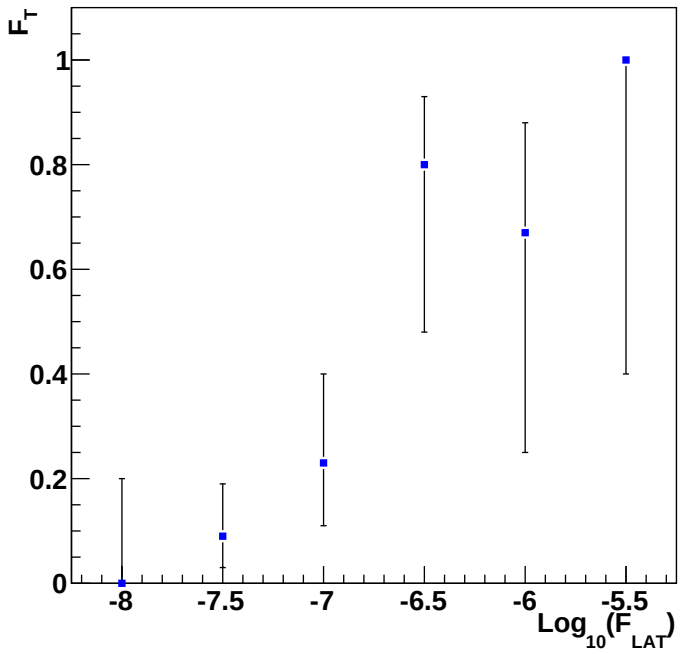

Figure 6: The fraction F_T (see text) of *Fermi-LAT* pulsars seen by Milagro as a function of half-decade bins of the integrated *Fermi-LAT* flux (photons $cm^{-2}s^{-1}$) in the energy range from 100 MeV to 100 GeV.

Table 1: Summary of the search with $\lambda = 0.01$ for TeV emission from the 2FGL list that are identified as candidates off the galactic plane. (Note that we used the same abbreviations for the source type as the 2FGL, agu = active galaxy of uncertain type, bzb = BL Lac type of blazar and bzq = FSRQ type of blazar.) The Milagro flux derived at 7 TeV is given for candidates that passed the $\lambda = 0.01$ FDR cut and 95% confidence level flux upper limit is given for the rest.

Fermi Name 2FGL	RA (deg)	DEC (deg)	l (deg)	b (deg)	Flux/Flux Limit ($\times 10^{-17}$TeV^{-1} s^{-1}cm^{-2})	Source Type	Significance σ	Associated source
J0007.8+4713	1.97	47.23	115.3	-15	< 65.06	bzb	-0.78	MG4 J000800+4712
J0009.1+5030	2.29	50.51	116.09	-11.8	< 85.8	agu	-0.26	NVSS J000922+503028
J0022.5+0607	5.64	6.12	110.02	-56.02	< 279.67	bzb	-0.1	PKS 0019+058
J0045.3+2127	11.34	21.45	121.04	-41.4	< 120.71	bzb	0.48	GB6 J0045+2127
J0100.2+0746	15.06	7.78	126.74	-55.03	< 378.43	bzb	1.69	GB6 J0100+0745
J0106.5+4854	16.65	48.91	125.49	-13.88	< 95.99		0.21	
J0108.6+0135	17.17	1.59	131.85	-60.98	< 566.7	bzq	0.64	4C 1.02
J0112.1+2245	18.03	22.76	129.15	-39.86	< 63.03	bzb	-1.29	S2 0109+22
J0112.8+3208	18.21	32.14	128.19	-30.51	< 48.2	bzq	-1.71	4C 31.03
J0115.4+0358	18.87	3.97	134.43	-58.37	< 296.62	bzb	-0.59	PMN J0115+0356
J0136.5+3905	24.14	39.09	132.42	-22.95	< 70.3	bzb	-0.46	B3 0133+388
J0136.9+4751	24.24	47.86	130.78	-14.32	< 117.84	bzq	0.89	OC 457
J0144.6+2704	26.16	27.08	137.29	-34.31	< 85.04	bzb	-0.03	TXS 0141+268
J0153.9+0823	28.49	8.4	148.21	-51.38	< 209.19	bzb	-0.2	GB6 J0154+0823
J0211.2+1050	32.81	10.84	152.59	-47.39	< 106.04	bzb	-1.48	MG1 J021114+1051
J0217.4+0836	34.35	8.61	156.17	-48.63	< 138.64	bzb	-1.14	ZS 0214+083
J0217.9+0143	34.48	1.73	162.2	-54.41	< 347.2	bzq	-0.84	PKS 0215+015
J0221.0+3555	35.27	35.93	142.6	-23.49	< 85.82	bzq	0.21	S4 0218+35
J0222.6+4302	35.66	43.04	140.14	-16.77	< 85.18	BZB	0.13	3C 66A
J0237.8+2846	39.47	28.78	149.48	-28.55	< 101.74	bzq	0.58	4C 28.07
J0238.7+1637	39.68	16.62	156.78	-39.1	< 131.21	BZB	0.24	AO 0235+164
J0316.1+0904	49.05	9.08	172.1	-39.59	< 339.0	bzb	1.59	GB6 J0316+0904
J0319.8+4130	49.97	41.51	150.58	-13.25	< 74.54	rdg	-0.15	NGC 1275
J0326.1+0224	51.55	2.41	180.74	-42.45	< 802.03	bzb	1.66	1H 0323+022
J0333.7+2918	53.43	29.31	160.49	-21.49	< 103.39	agu	0.62	TXS 0330+291
J0423.2-0120	65.81	-1.34	195.28	-33.15	< 1039.11	BZQ	1.35	PKS 0420-01
J0433.5+2905	68.39	29.09	170.52	-12.62	< 114.07	bzb	0.93	MG2 J043337+2905
J0442.7-0017	70.69	0.29	197.21	-28.44	< 863.75	bzq	1.04	PKS 0440-00
J0448.9+1121	72.24	11.36	187.4	-20.77	< 198.53	bzq	0.41	PKS 0446+11
J0508.0+6737	77.01	67.63	143.8	15.9	< 648.35	bzb	2.53	1ES 0502+675
J0509.4+0542	77.37	5.7	195.4	-19.62	< 320.94	bzb	0.34	TXS 0506+056
J0532.7+0733	83.19	7.56	196.84	-13.71	< 275.2	bzq	0.68	OG 50
J0534.8-0548c	83.72	-5.81	209.36	-19.66	< 942.7		-1.51	
J0541.8-0203c	85.45	-2.06	206.69	-16.41	< 1007.43		0.66	
J0547.1+0020c	86.8	0.34	205.15	-14.1	< 666.58		0.24	
J0607.4+4739	91.87	47.66	165.64	12.87	< 76.14	bzb	-0.4	TXS 0603+476
J0612.8+4122	93.21	41.37	171.83	10.92	< 86.2	bzb	0.24	B3 0609+413
J0650.7+2505	102.7	25.1	190.24	11.02	< 45.99	bzb	-2.17	1ES 0647+250
J0654.2+4514	103.57	45.24	171.2	19.36	< 77.21	bzq	-0.14	B3 0650+453
J0654.5+5043	103.65	50.72	165.68	21.14	< 164.55	bzq	1.79	GB6 J0654+5042
J0714.0+1933	108.51	19.57	197.68	13.61	< 103.44	bzq	-0.03	MG2 J071354+1934
J0719.3+3306	109.83	33.11	185.06	19.85	< 115.37	bzq	1.02	B2 0716+33
J0721.9+7120	110.48	71.35	143.97	28.02	< 512.3	bzb	0.49	S5 0716+71
J0725.3+1426	111.33	14.44	203.63	13.93	< 169.64	BZQ	0.49	4C 14.23
J0738.0+1742	114.52	17.7	201.85	18.06	< 152.56	bzb	0.83	PKS 0735+17

Table 1: Cont.. Summary of the search with $\lambda = 0.01$ for TeV emission from the 2FGL list that are identified as candidates off the galactic plane. (Note that we used the same abbreviations for the source type as the 2FGL, agu = active galaxy of uncertain type, bzb = BL Lac type of blazar and bzq = FSRQ type of blazar.) The Milagro flux derived at 7 TeV is given for candidates that passed the $\lambda = 0.01$ FDR cut and 95% confidence level flux upper limit is given for the rest.

Fermi Name 2FGL	RA (deg)	DEC (deg)	l (deg)	b (deg)	Flux/Flux Limit ($\times 10^{-17}$TeV^{-1} s^{-1}cm^{-2})	Source Type	Significance σ	Associated source
J0739.2+0138	114.82	1.65	216.96	11.39	< 293.61	bzq	-1.35	PKS 0736+01
J0805.3+7535	121.34	75.59	138.88	30.79	< 1032.12	bzb	-0.11	RX J0805.4+7534
J0807.1-0543	121.78	-5.72	227	13.99	< 1883.54	bzb	0.61	PKS 0804-05
J0809.8+5218	122.46	52.31	166.26	32.91	< 136.9	bzb	1.07	0806+524
J0818.2+4223	124.57	42.4	178.21	33.41	< 113.39	bzb	1.15	S4 0814+42
J0831.9+0429	127.99	4.49	220.72	24.36	< 417.64	bzb	0.4	PKS 0829+046
J0854.8+2005	133.71	20.1	206.83	35.83	< 93.21	BZB	-0.35	OJ 287
J0905.6+1357	136.4	13.96	215.04	35.96	< 190.04	bzb	0.88	MG1 J090534+1358
J0909.1+0121	137.29	1.37	228.93	30.92	< 576.86	bzq	0.19	PKS 0906+01
J0909.7-0229	137.43	-2.5	232.8	28.99	< 476.09	bzq	-1.54	PKS 0907-023
J0915.8+2932	138.96	29.54	196.67	42.93	< 134.29	bzb	1.58	B2 0912+29
J0920.9+4441	140.24	44.7	175.7	44.81	< 107.06	bzq	0.84	S4 0917+44
J0957.7+5522	149.43	55.38	158.59	47.94	< 86.48	bzq	-0.63	4C 55.17
J1012.6+2440	153.17	24.68	207.74	54.36	< 77.99	bzq	-0.37	MG2 J101241+2439
J1015.1+4925	153.79	49.43	165.53	52.73	< 124.22	bzb	1.04	1H 1013+498
J1016.0+0513	154.01	5.23	236.51	47.04	< 412.37	bzq	0.74	TXS 1013+054
J1033.9+6050	158.48	60.84	147.8	49.13	< 136.0	BZQ	-0.18	S4 1030+61
J1037.6+5712	159.42	57.21	151.77	51.77	< 89.82	bzb	-0.82	GB6 J1037+5711
J1058.4+0133	164.61	1.57	251.5	52.77	< 451.8	bzb	0.01	4C 1.28
J1058.6+5628	164.67	56.48	149.57	54.42	< 110.53	bzb	0.02	TXS 1055+567
J1104.4+3812	**166.12**	**38.21**	**179.82**	**65.03**	**389.74±40.7**	**bzb**	**9.57**	**Mkn 421**
J1117.2+2013	169.31	20.23	225.63	67.39	< 90.1	bzb	-0.45	RBS 958
J1121.5-0554	170.39	-5.91	266.27	50.45	< 2362.34	bzq	1.39	PKS 1118-05
J1132.9+0033	173.23	0.56	264.33	57.42	< 798.62	bzb	1.3	PKS B1130+008
J1150.5+4154	177.63	41.91	159.14	70.67	< 80.64	bzb	0.12	RBS 1040
J1159.5+2914	179.88	29.25	199.41	78.37	< 79.56	bzq	-0.11	Ton 599
J1217.8+3006	184.47	30.11	188.93	82.06	< 74.31	bzb	-0.25	1ES 1215+303
J1221.3+3010	185.35	30.18	186.33	82.74	< 77.42	bzb	-0.12	PG 1218+304
J1221.4+2814	185.37	28.24	201.69	83.28	< 113.67	bzb	0.9	W Comae
J1224.9+2122	186.23	21.38	255.07	81.66	< 168.32	BZQ	1.59	4C 21.35
J1226.0+2953	186.52	29.9	185.02	83.78	< 60.44		-0.87	
J1229.1+0202	187.28	2.04	289.95	64.35	< 459.81	BZQ	0.01	3C 273
J1231.7+2848	187.94	28.81	190.66	85.34	< 54.27	bzb	-1.28	B2 1229+29
J1239.5+0443	189.88	4.73	295.18	67.42	< 405.6	bzq	0.73	MG1 J123931+0443
J1243.1+3627	190.78	36.45	133.13	80.51	< 67.63	bzb	-0.45	Ton 116
J1248.2+5820	192.06	58.35	123.74	58.77	< 107.89	bzb	-0.44	PG 1246+586
J1253.1+5302	193.28	53.05	122.36	64.08	< 72.69	bzb	-0.99	S4 1250+53
J1256.1-0547	194.04	-5.79	305.1	57.06	< 1072.78	BZQ	-1.07	3C 279
J1303.1+2435	195.78	24.6	349.62	86.35	< 117.62	bzb	0.85	MG2 J130304+2434
J1309.4+4304	197.37	43.08	111.17	73.64	< 87.93	bzb	0.26	B3 1307+433
J1310.6+3222	197.67	32.38	85.59	83.29	< 65.29	bzq	-0.68	OP 313
J1312.8+4828	198.21	48.47	113.32	68.25	< 71.38	bzq	-0.57	GB 1310+487
J1418.4-0234	214.6	-2.57	341.56	53.64	< 1091.11	bzb	1.01	BZB J1418-0233
J1427.0+2347	216.76	23.8	29.48	68.2	< 96.03	bzb	0.13	PKS 1424+240
J1438.7+3712	219.68	37.21	63.72	65.27	< 50.77	bzq	-1.33	B2 1436+37B

Table 1: Cont.. Summary of the search with $\lambda = 0.01$ for TeV emission from the 2FGL list that are identified as candidates off the galactic plane. (Note that we used the same abbreviations for the source type as the 2FGL, agu = active galaxy of uncertain type, bzb = BL Lac type of blazar and bzq = FSRQ type of blazar.) The Milagro flux derived at 7 TeV is given for candidates that passed the $\lambda = 0.01$ FDR cut and 95% confidence level flux upper limit is given for the rest.

Fermi Name 2FGL	RA (deg)	DEC (deg)	l (deg)	b (deg)	Flux/Flux Limit ($\times 10^{-17}$TeV^{-1} s^{-1}cm^{-2})	Source Type	Significance σ	Associated source
J1454.4+5123	223.62	51.4	87.66	56.46	< 109.12	bzb	0.49	TXS 1452+516
J1501.0+2238	225.28	22.64	31.46	60.34	< 114.2	bzb	0.55	MS 1458.8+2249
J1504.3+1029	226.1	10.49	11.37	54.58	< 185.18	BZQ	0.0	PKS 1502+106
J1520.8-0349	230.22	-3.83	358.11	42.48	< 820.68	bzb	-0.48	NVSS J152048-034850
J1522.1+3144	230.54	31.74	50.18	57.02	< 101.94	bzq	0.64	B2 1520+31
J1542.9+6129	235.73	61.49	95.38	45.4	< 93.21	bzb	-1.34	GB6 J1542+6129
J1553.5+1255	238.39	12.93	23.77	45.21	< 109.28	bzq	-0.97	PKS 1551+130
J1555.7+1111	238.94	11.19	21.92	43.95	< 160.64	bzb	-0.17	PG 1553+113
J1607.0+1552	241.77	15.88	29.4	43.42	< 85.05	bzb	-1.16	4C 15.54
J1625.2-0020	246.3	0.33	13.92	31.83	< 762.2		0.66	
J1635.2+3810	248.81	38.17	61.13	42.34	< 58.66	bzq	-0.95	4C 38.41
J1637.7+4714	249.43	47.24	73.38	41.88	< 68.76	bzq	-0.6	4C 47.44
J1640.7+3945	250.18	39.76	63.35	41.38	< 122.41	BZQ	1.31	NRAO 512
J1642.9+3949	250.18	39.76	63.48	40.95	< 122.41	BZQ	1.31	3C 345
J1640.7+3945	250.75	39.83	63.35	41.38	< 115.23	BZQ	1.11	NRAO 512
J1642.9+3949	250.75	39.83	63.48	40.95	< 115.23	BZQ	1.11	3C 345
J1653.6-0159	253.4	-2	16.59	24.93	< 847.78		0.15	
J1653.9+3945	253.48	39.76	63.61	38.85	< 186.65	BZB	2.93	Mkn 501
J1700.2+6831	255.06	68.52	99.58	35.19	< 316.95	bzq	-0.1	TXS 1700+685
J1709.7+4319	257.45	43.32	68.41	36.21	< 113.14	bzq	1.01	B3 1708+433
J1719.3+1744	259.83	17.74	39.53	28.07	< 183.16	bzb	1.41	PKS 1717+177
J1722.7+1013	260.68	10.23	32.22	24.3	< 425.7	bzq	2.84	TXS 1720+102
J1725.0+1151	261.27	11.87	34.11	24.47	< 288.43	bzb	1.82	1H 1720+117
J1734.3+3858	263.58	38.98	64.04	31.02	< 95.96	bzq	0.48	B2 1732+38A
J1748.8+7006	267.22	70.11	100.54	30.69	< 275.01	bzb	-1.01	1749+70
J1751.5+0938	267.88	9.64	34.91	17.65	< 183.43	bzb	0.0	OT 81
J1754.3+3212	268.58	32.2	57.75	25.38	< 60.01	bzb	-0.97	RX J1754.1+3212
J1800.5+7829	270.15	78.48	110.06	29.07	< 1134.67	bzb	-0.91	S5 1803+784
J1806.7+6948	271.68	69.8	100.1	29.18	< 497.66	bzb	0.75	3C 371
J1811.3+0339	272.83	3.66	31.62	10.59	< 279.71	bzb	-0.73	NVSS J181118+034114
J1824.0+5650	276	56.84	85.72	26.09	< 65.02	bzb	-1.93	4C 56.27
J1838.7+4759	279.7	47.99	76.9	21.82	< 107.68	bzb	0.63	GB6 J1838+4802
J1849.4+6706	282.35	67.1	97.5	25.03	< 287.58	bzq	0.2	S4 1849+67
J1852.5+4856	283.13	48.94	78.6	19.94	< 41.8	bzq	-2.49	S4 1851+48
J1903.3+5539	285.84	55.67	85.96	20.51	< 77.36	bzb	-1.1	TXS 1902+556
J1927.0+6153	291.77	61.9	93.31	19.71	< 123.93	bzb	-0.79	1RXS J192649.5+615445
J2000.0+6509	300.02	65.16	98.02	17.67	< 208.54	bzb	-0.07	1ES 1959+650
J2116.2+3339	319.05	33.66	79.82	-10.64	< 124.07	bzb	1.32	B2 2114+33
J2121.0+1901	320.26	19.03	69.25	-21.25	< 168.15	bzq	1.26	OX 131
J2133.9+6645	323.49	66.75	105.17	10.96	< 316.94		0.47	
J2143.5+1743	325.88	17.72	72.09	-26.08	< 108.01	bzq	-0.21	OX 169
J2147.3+0930	326.84	9.51	65.85	-32.28	< 162.46	bzq	-0.35	PKS 2144+092
J2202.8+4216	330.71	42.27	92.6	-10.46	< 47.82	bzb	-1.53	BL Lacertae
J2203.4+1726	330.87	17.44	75.68	-29.63	< 164.9	bzq	0.9	PKS 2201+171
J2236.4+2828	339.1	28.48	90.12	-25.66	< 86.69	bzb	0.05	B2 2234+28A

Table 1: Cont.. Summary of the search with $\lambda = 0.01$ for TeV emission from the 2FGL list that are identified as candidates off the galactic plane. (Note that we used the same abbreviations for the source type as the 2FGL, agu = active galaxy of uncertain type, bzb = BL Lac type of blazar and bzq = FSRQ type of blazar.) The Milagro flux derived at 7 TeV is given for candidates that passed the $\lambda = 0.01$ FDR cut and 95% confidence level flux upper limit is given for the rest.

Fermi Name 2FGL	RA (deg)	DEC (deg)	l (deg)	b (deg)	Flux/Flux Limit ($\times 10^{-17}$TeV^{-1} s^{-1}cm^{-2})	Source Type	Significance σ	Associated source
J2243.9+2021	341	20.36	86.59	-33.37	< 84.11	bzb	-0.7	RGB J2243+203
J2244.1+4059	341.03	40.99	98.5	-15.77	< 100.26	bzb	0.69	TXS 2241+406
J2253.9+1609	343.5	16.15	86.12	-38.18	< 135.72	BZQ	0.23	3C 454.3
J2311.0+3425	347.77	34.43	100.42	-24.02	< 62.49	bzq	-0.78	B2 2308+34
J2323.6-0316	350.91	-3.28	77.78	-58.23	< 552.24	bzq	-1.9	PKS 2320-035
J2323.8+4212	350.95	42.2	106.06	-17.78	< 81.89	bzb	0.13	1ES 2321+419
J2325.3+3957	351.33	39.96	105.52	-19.98	< 47.82	bzb	-1.62	B3 2322+396
J2334.8+1431	353.72	14.53	96.56	-44.39	< 167.75	bzb	0.7	BZB J2334+1408
J2339.6-0532	354.91	-5.54	81.36	-62.47	< 2061.09		0.84	

Table 2: Summary of the search with $\lambda = 0.01$ for TeV emission from the TeVCat list that are identified as candidates off the galactic plane. (Note that: HBL = High Frequency Peaked BL Lac, IBL = Intermediate Frequency Peaked BL Lac, LBL = Low Frequency Peaked BL Lac, UNID = Unidentified, FSRQ = Flat Spectrum Radio Quasar, AGN = Active Galactic Nuclei, Cat. Var. = Cataclysmic Variable Star and FR I = Fanaroff-Riley Type I radio source.) The Milagro flux derived at 7 TeV is given for the candidates that passes the $\lambda = 0.01$ FDR cut and 95% confidence level upper limits given for the rest.

Name	RA (deg)	DEC (deg)	l (deg)	b (deg)	Flux/Flux Limit ($\times 10^{-17}$TeV^{-1} s^{-1}cm^{-2})	Source Type	Significance σ	2FGL Association 2FGL
RGB J0152+017	28.1396	1.77786	152.34317	-57.561295	$<$ 467.36	HBL	0.04	
3C66A	35.6733	43.0432	140.24803	-16.753392	$<$ 85.18	IBL	0.13	
3C66A/B	35.8	43.0117	140.24803	-16.753392	$<$ 83.18	UNID	0.06	
1ES 0229+200	38.2217	20.2725	152.97002	-36.612512	$<$ 81.55	HBL	-0.8	
IC 310	49.1792	41.3247	150.57567	-13.261242	$<$ 76.53	AGN	-0.12	
NGC 1275	49.9504	41.5117	150.57567	-13.261242	$<$ 74.54	FRI	-0.15	
RBS 0413	49.9658	18.7594	165.10684	-31.69731	$<$ 97.2	HBL	-0.4	
1ES 0414+009	64.2184	1.09008	191.81416	-33.159267	$<$ 478.08	HBL	-0.36	
1ES 0502+675[7]	76.9842	67.6233	143.795	15.88981	$<$ 651.78	HBL	2.55	
RGB J0710+591	107.61	59.15	157.39076	25.420975	$<$ 146.09	HBL	0.31	
S5 0716+714	110.473	71.3433	143.9812	28.017623	$<$ 512.3	LBL	0.49	
1ES 0806+524	122.496	52.3167	166.24607	32.93548	$<$ 136.9	HBL	1.07	
M82	148.97	69.6794	141.4095	40.567564	$<$ 343.13	Starburst	-0.35	
1ES 1011+496	153.767	49.4336	165.53394	52.712223	$<$ 124.22	HBL	1.04	
Markarian 421	**166.079**	**38.1947**	**179.88395**	**65.01015**	**395.08±40.69**	**HBL**	**9.7**	
Markarian 180	174.11	70.1575	131.90989	45.641234	$<$ 362.44	HBL	-0.15	
1ES 1215+303	184.467	30.1169	188.87483	82.052923	$<$ 74.31	LBL	-0.25	
1ES 1218+304	185.36	30.1914	186.20601	82.743376	$<$ 77.42	HBL	-0.12	
W Comae	185.382	28.2331	201.735	83.288032	$<$ 113.67	IBL	0.9	
4C +21.35	186.227	21.3794	255.07319	81.65946	$<$ 168.32	FSRQ	1.59	
M87	187.697	12.3975	283.73831	74.494439	$<$ 115.55	FRI	-1.02	
3C279	194.046	-4.21056	305.20657	58.640166	$<$ 1212.26	FSRQ	-0.11	
PKS 1424+240	216.752	23.8	29.487026	68.207689	$<$ 96.03	IBL	0.13	
H 1426+428	217.136	42.6725	77.487039	64.899104	$<$ 79.44	HBL	-0.04	
1ES 1440+122	220.701	12.0111	8.3294143	59.840034	$<$ 96.45	IBL	-1.62	
PG 1553+113	238.936	11.1947	21.918776	43.960313	$<$ 160.64	HBL	-0.17	
Markarian 501[8]	253.468	39.7603	63.600083	38.859361	$<$ 186.65	HBL	2.93	
1ES 1959+650	299.999	65.1486	98.003397	17.670031	$<$ 209.2	HBL	-0.06	
AEAquarii	310.042	0.871111	46.934522	-23.552194	$<$ 446.02	Cat._Var.	-0.53	
BL Lacertae	330.68	42.2778	92.589572	-10.441029	$<$ 48.15	LBL	-1.51	
B3 2247+381	342.528	38.4328	98.267934	-18.559532	$<$ 84.69	HBL	0.14	

Table 3: Summary of the search with $\lambda = 0.01$ for TeV emission from the pulsars in the 2FGL list that were not listed in the 0FGL. (Note that we used the same abbreviations for the source type as the 2FGL: PSR = Pulsar identified by pulsations and psr = Pulsar identifies by spatial association.) The Milagro flux derived at 35 TeV is given for the candidates that passed the $\lambda = 0.01$ FDR cut and 95% confidence level upper limits are given for the rest.

Fermi Name 2FGL	RA (deg)	DEC (deg)	l (deg)	b (deg)	Flux/Flux Limit ($\times 10^{-17}$TeV^{-1} s^{-1}cm^{-2})	Source Type	Significance σ	Associated source
J0023.5+0924	5.89	9.41	111.5	-52.85	$<$ 22.42	psr	-0.73	PSR J0023+09
J0034.4-0534	8.61	-5.58	111.55	-68.08	$<$ 54.58	PSR	-2.06	PSR J0034-0534
J0102.9+4838	15.74	48.65	124.9	-14.18	$<$ 22.31	psr	0.51	PSR J0103+48
J0205.8+6448	31.45	64.81	130.74	3.07	$<$ 20.75	PSR	-0.88	PSR J0205+6449
J0218.1+4233 [9]	34.53	42.55	139.5	-17.51	$<$ 41.80	PSR	2.94	PSR J0218+4232
J0248.1+6021	42.04	60.36	136.89	0.69	$<$ 38.32	PSR	1.54	PSR J0248+6021
J0308.3+7442	47.08	74.71	131.73	14.23	$<$ 53.95	psr	-0.15	PSR J0308+7442
J0340.4+4131	55.1	41.53	153.78	-11.01	$<$ 14.87	PSR	-0.52	PSR J0340+4130
J0659.7+1417	104.93	14.29	201.05	8.27	$<$ 37.31	PSR	1.18	PSR J0659+1414
J0751.1+1809	117.78	18.15	202.7	21.09	$<$ 19.51	PSR	-0.43	PSR J0751+1807
J1023.6+0040	155.92	0.68	243.43	45.78	$<$ 43.66	psr	-0.33	PSR J1023+0038
J1142.9+0121	175.74	1.35	267.56	59.44	$<$ 37.41	psr	-0.9	PSR J1142+01
J1301.5+0835	195.39	8.58	310.76	71.3	$<$ 21.62	psr	-0.82	PSR J1301+08
J1312.7+0051	198.18	0.85	314.82	63.23	$<$ 58.01	psr	0.5	PSR J1312+00
J1549.7-0657	237.43	-6.96	1.23	35.03	$<$ 88.75	psr	-0.8	PSR J1549-06
J1714.0+0751	258.5	7.86	28.84	25.21	$<$ 18.13	PSR	-1.58	PSR J1713+0747
J1745.6+1015	266.4	10.27	34.84	19.23	$<$ 32.77	psr	0.48	PSR J1745+10
J1810.7+1742	272.69	17.7	44.62	16.76	$<$ 18.39	psr	-0.6	PSR J1810+17
J1846.4+0920	281.61	9.34	40.7	5.34	$<$ 23.81	PSR	-0.54	PSR J1846+0919
J1928.8+1740c	**292.22**	**17.68**	**52.87**	**0.03**	**46.41±11.50**	**psr**	**4.03**	**PSR J1928+1746**
J1957.9+5033	299.48	50.56	84.61	10.98	$<$ 28.56	PSR	1.41	PSR J1957+5033
J1959.5+2047	299.9	20.79	59.18	-4.7	$<$ 15.32	PSR	-0.85	PSR J1959+2048
J2030.0+3640	**307.51**	**36.68**	**76.12**	**-1.45**	**42.68±9.55**	**PSR**	**4.46**	**PSR J2030+3641**
J2017.3+0603	304.35	6.05	48.63	-16.02	$<$ 27.2	PSR	-0.71	PSR J2017+0603
J2043.2+1711	310.81	17.18	61.9	-15.3	$<$ 17.82	PSR	-0.76	PSR J2043+1710
J2043.7+2743	310.95	27.72	70.65	-9.14	$<$ 14.62	PSR	-0.72	PSR J2043+2740
J2046.7+1055	311.69	10.93	57.02	-19.57	$<$ 37.49	psr	0.99	PSR J2047+10
J2129.8-0428	322.47	-4.48	48.93	-36.96	$<$ 104.35	psr	0.55	PSR J2129-04
J2215.7+5135	333.94	51.59	99.89	-4.18	$<$ 13.28	psr	-1.1	PSR J2215+51
J2234.7+0945	338.69	9.75	76.29	-40.43	$<$ 31.44	psr	0.38	PSR J2234+09
J2238.4+5902	**339.61**	**59.05**	**106.55**	**0.47**	**50.41±11.10**	**PSR**	**4.53**	**PSR J2238+5903**
J2239.8+5825 [10]	339.97	58.43	106.41	-0.16	$<$ 51.39	PSR	3.01	PSR J2240+5832

Table 4: Summary of the FDR thresholds and trials corrections for all the candidate lists with different λ

Candiate List	Pulsar List	2FGL Extragalactic List	TeVCat Extragalactic List
FDR Threshold with $\lambda = 0.1$	2.08 σ	3.45 σ	2.23 σ
Trials Correction with $\lambda = 0.1$	2.73 σ	3.63 σ	2.72 σ
FDR Threshold with $\lambda = 0.05$	2.35 σ	3.63 σ	2.58 σ
Trials Correction with $\lambda = 0.05$	2.95 σ	3.80 σ	2.94 σ
FDR Threshold with $\lambda = 0.01$	3.02 σ	4.03 σ	3.21 σ
Trials Correction with $\lambda = 0.01$	3.42 σ	4.18 σ	3.41 σ
FDR Threshold with $\lambda = 0.001$	3.66 σ	4.54 σ	3.82 σ
Trials Correction with $\lambda = 0.001$	4.00 σ	4.68 σ	3.99 σ

References

[1] Abdo, A. A., et al. 2007, *ApJ. Lett.*, 664, L91
[2] Abdo, A. A., et al. 2009a, VizieR Online Data Catalog, 218, 30046
[3] Abdo, A. A., et al. 2009b, *ApJ. Lett.*, 700, L127
[4] Abdo, A. A., Allen, B. T., Atkins, R., et al. 2012, *ApJ.*, 750, 63
[5] Abdo, A. A., Abeysekara, U., Allen, B. T., et al. 2012, *ApJ.*, 753, 159
[6] Abeysekara, A. U., Aguilar, J. A., Aguilar, S., et al. 2012, Astroparticle Physics, 35, 641
[7] Acciari, V. A., Aliu, E., Arlen, T., et al. 2010, *ApJ. Lett.*, 719, L69
[8] Acciari, V. A., Aliu, E., Arlen, T., et al. 2011a, *ApJ.*, 738, 25
[9] Acciari, V. A., Arlen, T., Aune, T., et al. 2011b, *ApJ.*, 729, 2
[10] Afanas'Ev, V. L., Dodonov, S. N., Moiseev, A. V., et al. 2005, Astronomy Reports, 49, 374
[11] Aharonian, F., et al. 2006, *ApJ.*, 636, 777
[12] Albert, J., Aliu, E., Anderhub, H., et al. 2007, *ApJ.*, 663, 125
[13] Atkins, R., Benbow, W., Berley, D., et al. 2004, *ApJ.*, 608, 680
[14] Bartoli, B., Bernardini, P., Bi, X. J., et al. 2012, *ApJ. Lett.*, 745, L22
[15] Costamante, L., & Ghisellini, G. 2002, *A.& A.*, 384, 56
[16] Dwek, E., & Krennrich, F. 2005, *ApJ.*, 618, 657
[17] Gast, H., Brun, F., Carrigan, S., et al. 2011, International Cosmic Ray Conference, 7, 157
[18] Goodman, J., & Sinnis, G. 2009, The Astronomer's Telegram, 2172, 1
[19] Helene, O. 1983, Nuclear Instruments and Methods in Physics Research, 212, 319
[20] Krennrich, F., et al. 2001, *ApJ. Lett.*, 560, L45
[21] Kurczynski, P., & Gawiser, E. 2010, *AJ.*, 139, 1592
[22] Miller, C. J., et al. 2001, *AJ.*, 122, 3492
[23] Nolan, P. L., Abdo, A. A., Ackermann, M., et al. 2012, *ApJS*, 199, 31
[24] Quinn, J., Akerlof, C. W., Biller, S., et al. 1996, *ApJ. Lett.*, 456, L83
[25] Wakely, S. P., & Horan, D. 2008, International Cosmic Ray Conference, 3, 1341